Research Article | Open Access

Validation of an Experimental Animal Model for Corneal Additive Surgery

Lucía Ibares-Frías[1-3]*, Patricia Gallego[1,4], Roberto Cantalapiedra-Rodriguez[4], Maria Cruz Valsero[1,5], Santiago Mar[1], Jesús Merayo-Lloves[1,6] and Maria Carmen Martínez-García[1,4]

[1]Group of Optical Diagnostic Techniques, University of Valladolid, Valladolid, Spain

[2]Instituto de Oftalmobiología Aplicada (IOBA), University of Valladolid, Valladolid, Spain

[3]Ophthalmology Department, Hospital Clínico Universitario de Valladolid, Valladolid, Spain

[4]Cell Biology, Histology and Pharmacology Department, University of Valladolid, Valladolid, Spain

[5]Biostatistics Department, University of Valladolid, Valladolid, Spain

[6]Fundación de Investigación Oftalmológica, Instituto Oftalmológico Fernandez Vega, Oviedo, Spain

*Corresponding author: Lucía Ibares-Frías, Departamento de Histología, Biología Celular y Farmacología, Facultad de Ciencias de la Salud, Universidad de Valladolid, Avenida Ramón y Cajal 7 47003, Valladolid, Spain, Tel: 0034658944269; Email: luciaibares@hotmail.com

Abstract

Purpose: To assess the hen cornea as a model for training and future wound healing studies after implantation of intrastromal corneal ring segments (ICRS) by clinical and optical outcomes.

Setting: University of Valladolid, Valladolid, Spain.

Design: Experimental study.

Methods: One 90°, 150-μm thick polymethyl methacrylate Ferrara ICRS segment was manually implanted at 70-80% depth of 192 Gallus domesticus corneas. Clinical follow-up for 6 months included monitoring corneal thickness, epithelial wound closure, edema, haze, and the location and severity of deposits. The refractive state was also measured. After each animal was euthanized, corneas were processed for direct transmittance and histological analysis.

Results: Complications were present in 16% of the eyes. Epithelial wound closure was completed at 3 ± 2 days. A slight corneal edema in the channel site was present for the first 15 days. All corneas had deposits by 4 months located along the inner, outer curvatures and under the segments. Corneal haze was present only at the incision site. ICRS induced hyperopic changes in the refractive state without changes in direct transmitance of central cornea. New cells and extracellular matrix were present around the segment where deposits were seen on clinical follow-up.

Conclusions: With hen as an animal model, ICRS were implanted in a precise and reproducible way after a learning curve. Similar to humans, the follow-up period during the first 6 months after implantation showed fast wound closure, deposits, and haze at the incision site. ICRS in hens also reduced the refractive power without affecting the central cornea.

Keywords: Experimental animal model; Intrastromal corneal ring segments; Corneal wound healing; Keratoconus; Deposits.

Introduction

Corneal ectatic disorders such as keratoconus, pellucid marginal degeneration, and post-laser-assisted in-situ keratomileusis ectasia, are a group of diseases characterized by progressive corneal thinning with an irregular increase in the corneal refractive power [1]. These alterations result in mild-to-marked impairment in the quality of vision. Corneal ectatic disease is a common problem facing the corneal ophthalmologist [1]. In the past, the first option for treating these disorders was contact lens wear. If this approach was not successful, then the only other option was keratoplasty [2]. However there are now different options before resorting to this surgery, such as cross-linking [3], implantation of an intrastromal corneal ring segment (ICRS) [4,5] and lamellar keratoplasty techniques[1].

The Ferrara ICRS is widely used throughout the world, with long-term follow-up studies [5,6]. There are other types of ICRSs, including the FDA-approved ICRS-INTACSTM with which the majority of published studies are performed [7-10]. The main difference between these two ICRSs is in the trasverse profile, the Ferrara ICRS is triangular while the INTACSTM is hexagonal [4,5,8].

ICRS surgery has some advantages over other keratorefractive techniques and other treatments for ectatic disorders. For instance, it does not cause any surgical damage to the central cornea; thus, the normal prolate corneal profile with concomitant reduction of the central corneal curvature is maintained. Additionally, the refractive effect is potentially reversible, as has been shown in some clinical studies [9,10]. Nevertheless, some complications with this technique

have been described, although the incidence is very low once the surgeon's learning curve has been completed [6,11-13]. Common complications described include extrusion, [12,14] infection, [11] ICRS migration and misplacement, [15] over- and under-correction, [9] halos and glare, [16] periannular opacities, [7,17] and neovascularization [13,15]. Many studies have analyzed the complications in humans, but most are based on statistical analyses without any histopathological explanation.

Deposits around the segments, seen on biomicroscopic examination, have been described as a complication in some studies, but the composition and evolution of these deposits has not been completely explained. Thus, despite the studies carried out with confocal microscopy, [17] optical coherence tomography, [18,19] and scanning electron microscopy of ICRS explanted from live patients, [12] little data is available regarding the correlation of clinical changes with histopathological changes. Ethical limitations make impossible to carry out these studies in humans and for this reason it is necessary to develop an experimental animal model. The use of an experimental animal model could provide the opportunity for training in surgery and to study together the optical, clinical and histological events that occur during the wound healing process. Pig eyes have commonly been used for surgical practice, but the difficulty in manipulating the living animal, along with the expensive cost and the anatomical differences with human corneas also make it difficult to use them as a model for studying the evolution process. The rabbit has been used as an experimental model too, [7] but differences exist compared to humans in anatomy, biomechanical properties as well as in the healing process which could compromise outcomes. For all of the above reasons, we propose the hen (adult chicken) model as an experimental model for the development of the learning curve of ICRS implantation and the study of the clinical and histological outcomes.

The aim of this study was to determine if chickens could serve as a suitable animal model to reproduce the learning curve of ICRS implantation surgery, and then, to follow the clinical and histopathological evolution of the cornea after ICRS implantation in normal and complicated eyes. Chickens are advantageous for this type of study because they are inexpensive, easy to handle, and the corneal anatomy and wound healing response [20,21] are similar to those of humans. Here we report the learning curve with complications and the clinical, refractive and optical changes that follow ICRS surgery in hens.

Material and Methods

Animals

Iber Braun adult hens (n=96), *Gallus gallus domesticus*, weighing about 2.5 kg each were used for ICRS implantation. The Animal Ethics Committee at the University of Valladolid approved the animal studies described in this research. The animals were cared for following the guidelines of the Association for Research in Vision and Ophthalmology (ARVO) Statement for the Use of Animals in Ophthalmic and Vision Research. The animals without complications were randomized into eleven groups with respect to sacrifice time and histological analysis.

Intrastromal segment implantation surgery

We implanted one Ferrara ICRS (FerraRing, AJL Ophthalmics, Vitoria, Spain) in each eye. The segments were made of polymethyl methacrylate (PMMA) and were triangular shaped in cross-section. They were 0.15 mm in thickness with a base of 600 μm, arc length of 90°, inner diameter of 4.4 mm, and outer diameter of 5.6 mm.

The surgery was carried out according to the method specified by Ferrara [4,14] while the hens were under general anaesthesia. All of the surgical procedures were performed by the same surgeon (LIF). The hens were anesthetized with an intramuscular injection of ketamine hydrochloride (37.5 mg/kg; Ketolar, Parke Davis SA, Barcelona, Spain) and xylazine hydrochloride (5 mg/kg; Rompun, Bayer, Leverkusen, Germany) followed by topical application of 0.5% tetracaine hydrochloride and 1 mg of oxybuprocaine (Colircusi Anestésico Doble, Alconcusí SA, Barcelona, Spain).

A wire lid speculum was positioned to keep the eye open during surgery. A circular Ferrara marker, previously dyed with a sterile gentian violet pen and centered where the microscope light was reflected on the cornea, was used to draw three concentric circles measuring 3, 5, and 7 mm in diameter on the cornea. The corneal thickness was measured at the incision site by ultrasonic pachymetry (Corneo-Gage Plus, Sonogage Inc., Cleveland, OH, USA). Using an adjustable Ferrara diamond blade knife, an incision was made through 70-80% of the corneal thickness at the 6 o´clock position between the 5- and 7 mm marked circles. A corneal bag was then made using a Suarez Spreader to facilitate the beginning of the channel preparation. A Ferrara spatula, modified for the chicken cornea (5 mm diameter) was inserted into the bag, and a semicircular channel was made in the stroma in a clockwise direction for right eyes and anticlockwise direction for left eyes. An ICRS was implanted into each channel. The segments were located in the inferotemporal quadrant in both eyes.

Clinical course

The corneas and anterior chamber of the eyes were evaluated under a surgical microscope (M220 F12, Leica Microsystems, Nussloch, Germany) before and after ICRS implantation. The animals were observed at 24, 48, and 72 hours, 7 and 15 days, and at 1-6 months. During the follow-up period, clinical signs were monitored. Corneal thickness was measure by pachymetry as described above. Epithelial wound closure was assessed with sodium fluorescein (Fluotest®, Alcon Cusi, Barcelona) every 8 hours until complete closure. Edema in the central cornea, incision site, channel around the segment, and in the residual channel through which the segment was passed during insertion was assessed as absent, minimum, medium, moderate, and severe and graded on a scale of 0-4. Deposits that developed in association with the segments were graded on the Ruckhofer scale [22] that ranged from 0 for no deposits to 4 for severe, fully confluent deposits that included the entire channel width and upon diffuse illumination did not allow visualization of the underlying structures. Haze was also graded on a 1-4 scale according to Fantes [23]. The presence of complications like corneal neovascularization, abscess, infiltrates, melting corneal ulcers, and extrusions was also described.

Refractive state

The refractive state was evaluated with an automated eccentric infrared photorefractor optimized by Schaeffel for measurements in chickens (Figure 1) [24,25]. The most hyperopic value at which the retinal reflex was reversed was taken to be the resting refraction. Refractive state measurements were taken pre-operatively and at 1-6 months after implantation. All were taken with the animals awake and under natural viewing conditions. Only refractive measurements of

hens without complications were included in the statistical analysis of refraction.
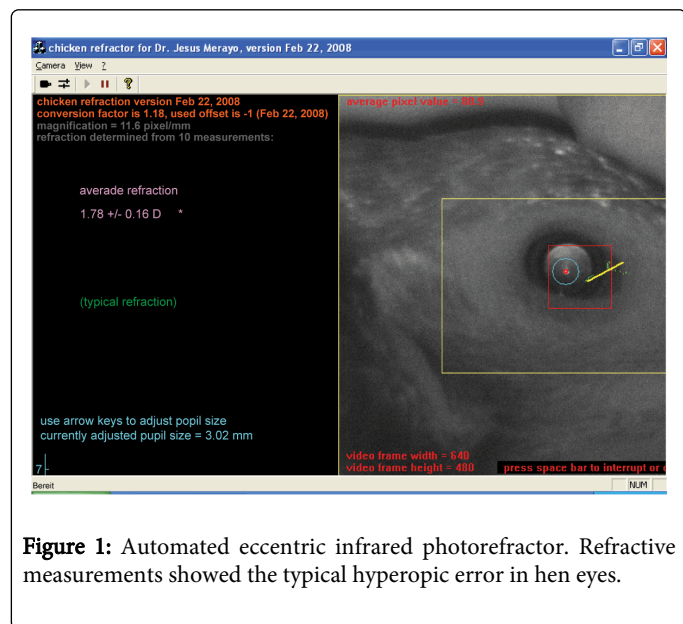

Figure 1: Automated eccentric infrared photorefractor. Refractive measurements showed the typical hyperopic error in hen eyes.

Direct corneal transmittance

For these and the following measurements and assessments, the eyes were enucleated from animals euthanized by an intracardiac injection of sodium pentobarbital (Dolethal® 0737-ESP Vetoquinol, Madrid, Spain) while under general anesthesia induced by ketamine and xylazine as described above. Only eyes with good follow-up were used for optical and histological measurements.

Measurements of light transmittance were taken immediately after animal sacrifice at 1, 3 and 6 months. The excised cornea was placed in a cornea holder filled with Ringer lactate (Frenesius Kabi España, S. A., Barcelona, Spain) at a constant temperature and continuous flow. Red light (632.8 nm) transmission across the cornea was measured by a Scatterometer (Optics Laboratory, University of Valladolid, Valladolid, Spain) [26].

Tissue processing and light microscopy

The eyes without complications were enucleated at 4, 12, 24, 48, and 72 hours, 7 days, and 1, 2, 3, 4, and 6 months after ICRS implantation. The eyes with complications were enucleated when they presented the complication. Then the eyes were fixed with 10% buffered formalin and embedded in paraffin wax. Later, the fixated eyes were sectioned into to hemispheres through the ICRS, leaving one half of each side segment. Then, parallel sagital sections of 7 μm thick were made through the two parts of the PMMA segment under the dissected microscope. Sections were stained with Carracci haematoxylin-eosin (H-E). For histological analysis, the sections were examined under an Olympus BX41 microscope (Olympus Life Science, Hamburg, Germany).

Statistical analysis

Statistical analysis was performed using the Statistical Package for the Social Sciences (SPSS v20, SPSS Inc., Chicago, IL, USA). Means and standard deviations were calculated for continuous variables. Independent Student's t-test was used for comparisons between two groups, and analysis of variance (ANOVA) was used for comparisons between more than two groups. P-values less than 0.05 were considered statistically significant.

Results

Clinical course and complications

The pre-operative central and peripheral corneal thicknesses measured by ultrasound pachymetry were 254 ± 42.7 μm (Table 1) and 342 ± 35.7 μm respectively. The average depth of the incision was 243.7 ± 24.0 μm, which was 71% of the peripheral corneal thickness.

	Preop	24 hours	48 hours	72 hours	7 days	1 Month	2 Months	3 Months	4 Months	5 Months	6 Months
Average of CT (μm) ± SD	254 ± 42.7	284.2 ± 82.9	286.3 ± 89.7	287.7± 92.1	285.8± 35.9	249.8± 17.7	248.3± 54.8	232.2 ± 78.1	227.7 ± 81.9	230.5 ± 49.5	235.6 ± 0.46
n	158	130	116	102	88	74	60	45	30	15	15
CT: corneal thickness, SD: standar deviation, n: number of eyes.											

Table 1: Pre and post ICRS implantation central pachymetry measurements.

The ICRS was successfully implanted in 98% of the eyes (188/192). Intraoperative adverse events were observed in 4 eyes (4/192, 2.1%). In 2 eyes a posterior corneal microperforation into the anterior chamber occurred because of a calibration mistake in the knife setting (Figure 6A); the other 2 eyes, had anterior corneal surface perforation. All this 4 surgeries were discontinued and healed without any complication. All these perforations occurred in the first surgeries.

Postoperative complications occurred in 16% of the implantations (30/188 eyes). Among the complications, 10.6% (20 eyes) were extrusions (Figure 2A), 3.2% (6 eyes) were corneal neovascularizations (Figure 2B and Figure 6B), 1.1% (2 eyes) were infiltrates (Figure 2C and Figure 6C), and 1.1% (2 eyes) were abscesses. The majority of these postoperative complications happened in the first 50 surgeries during the adaptation of the material to hens and the learning curve of the surgeon. 158 eyes had no complications and were used for clinical, refractive and optical studies. Fourteen corneas without complications were examined histologically at 4, 12, 24, 48, 72 hours, 7 days and 1 motnh. Fifteen corneas were examined histologically at 2, 3, 4 and 6 months. Corneas with complications were analyzed when they presented the complication.
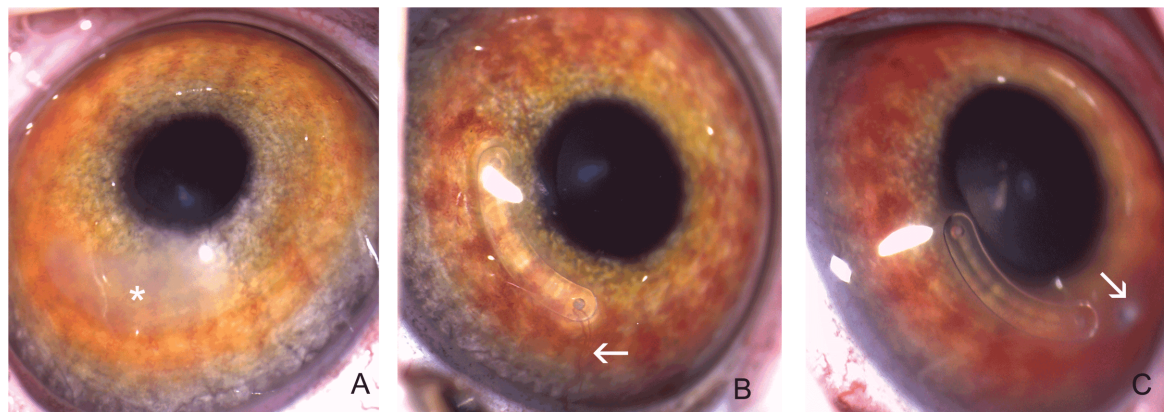
Figure 2: Clinical photographies of complications. A: Clinical photograph showing a difuse leucoma in the segment site secondary to spontaneous extrusion of the segment. B: Clinical phothograph of superficial neovascularization to the edge of the segment close to the incision (arrow). C: Clinical photograph showing an infiltrate in the incision site (arrow).

Epithelial wound closure measured by fluorescein staining

The incision morphology was diffuse at 24 hours (Figure 3A), and changed to a fish-mouth shape at 24-48 hours (Figure 3B). From 2 days, it took a linear form (Figure 3C). Complete closure, as indicated by the absence of fluorescein staining, was achieved by 3 ± 2 days.
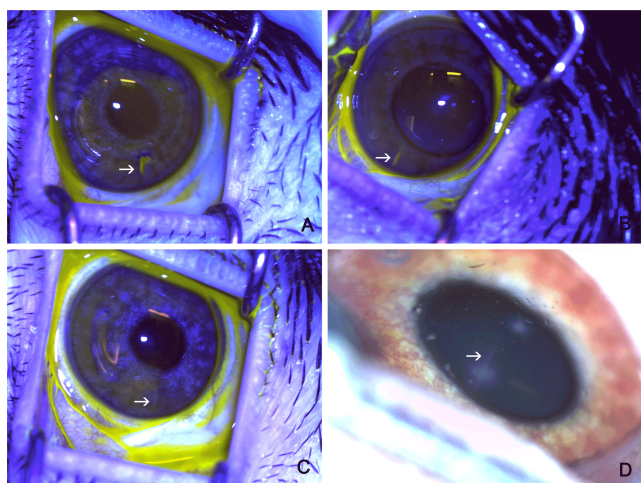

Figure 3: Time-dependent changes in the morphology of the incision (arrow: incision location). (A) Staining by fluorescein at 24 hours showed a diffuse incision site. (B) At 1-2 days, the incision site was shaped like a fish mouth. (C) On day 3, the incision site was linear. (D) At 3 months after insertion, the wound site appeared as a linear haze. Panels A-C, fluorescein staining. Panel D, clinical photograph.

Corneal edema

After ICRS implantation, there was slight corneal edema around the incision and at the stromal channel. It subsided spontaneously and was completely resolved by 7 days after surgery in the majority of the eyes (86%). Edema in the central cornea was measured by corneal ultrasound pachymetry. The thickness increased during the 7 days after ICRS insertion, but by 1 month it had decreased to pre-operative values (Table 1) and was maintained until the last follow up at 6 months. Central corneal edema was present at 1 month only in cases with complications.

Intrastromal deposits around segments

Deposits located in the empty space between the segment and the stroma where it was implanted (Figure 4A). In 28.4% of the eyes (25/88 eyes analized), intrastromal deposits first appeared in the positioning holes and along the inner curvature of the segments at day 7 after surgery (Figure 4B). By day 15, additional deposits were apparent at the outer curvature in 63.5% of the eyes (47/74). At 1 month, 94.5% of the eyes (70/74) had deposits that were under the segment in addition to the previously identified locations (Figure 4C). At 3 and 4 months, the deposits were present in 95.5% (43/45) and 100% (30/30) of the eyes respectively (Figure 4D).

The severity of the deposits was measured by the Ruckhofer normalized scale. The severity increased until 3 months. At 7 and 15 days, only trace deposits were observed, and they were fairly easy to differentiate from intrastromal corneal haze (Figure 4B). These deposits then increased in number and became more rounded and larger in size (grade 1 deposits) at 1 and 2 months (Figure 4C). Later, at 3 and 4 months, they were grades 2 and 3; more confluent and closer to the edges of the segments (Figure 4D). At 6 months the deposits were present in areas with corneal haze. They were smaller and less confluent than in previous months, like grade 1 deposits, especially along the inner curvature of the segment and under the segment. No grade 4 deposits were observed.

Corneal haze

Corneal haze was present at the incision site since the closure of the incision wound. It then increased in severity and decreased in size, becoming a thin line until the end of the study (Figure 3D-white arrow). No central corneal haze was observed in normal follow-up corneas.
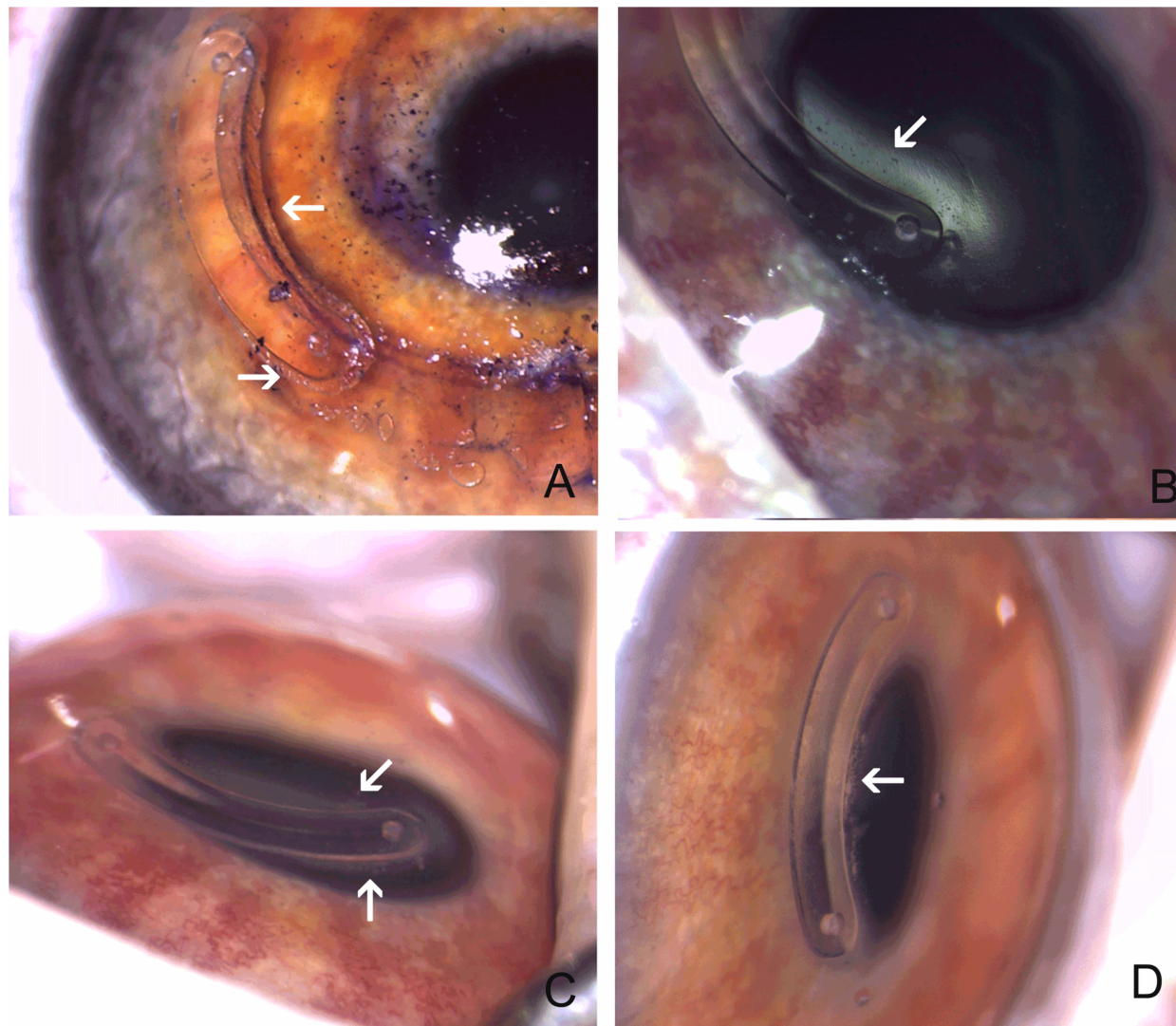
Figure 4: Changes in intrastromal deposits at different time points. (A) After implantation, there was an empty void between the segment and the stroma (arrows). (B) At 7 days, small, white deposits appeared along the inner curvature of the segment (arrow). (C) At 1 month, the deposits increased in number and were more rounded, bigger, and pigmented. They were located along the inner and outer curvatures of the segment and under the segment (arrows). (D) At 3 months, the deposits were bigger, more confluent and were closer to the segment (arrow).

	1 Month	3 Months	6 Months
DT	92.66 ± 1.5	92.1 ± 1.7	93.8 ± 3.74
n	9	6	5
DT: Direct transmittance, n: number of eyes			

Table 2: Direct transmittance (DT).

Direct transmittance

The direct transmittance values of the central cornea without reflection in no complicated eyes were represented in Table 2; 92, 66 ± 1.5 (9 eyes) at 1 month, 92.1 ± 1.7 (6 eyes) at 3 months and 93.8 ± 3.74 (5 eyes) at 6 months, without statistically differences (p>0.05) to control corneas (96 ± 1.08). At no time it was thought to have affected animals visual outcome.

Refractive error

Before ICRS implantation, all of the hens exhibited moderate hyperopic refractive errors (Table 3). The pre-operative mean refractive error was 4.40 ± 0.77 diopters (D). By one month after ICRS implantation, the refractive error, 7.25 ± 0.80 D, was statistically significant more hyperopic (*: p<0.05) than the pre-operative values. This change was maintained until the last follow-up at 6 months.

	Preop	1 Month	2 Months	3 Months	4 Months	5 Months	6 Months
Refractive error (D)	4.40 ± 0.77	7.25 ± 0.80*	7.39 ± 1.10*	7.06 ± 0.70*	7.35 ± 0.57*	7.53 ± 0.76*	7.54 ± 0.46*
n	188	74	60	45	30	15	15
D: diopters, n: number of eyes; *: p<0.05 compared to pre-operative value.							

Table 3: Pre- and post-ICRS implantation refractive error.

Histological findings

H-E staining: At 1 day after surgery, the epithelial thickness over the segment was decreased (Figure 5, arrow) compared to the epithelial thickness in cornea not afected by the segment, and was maintained until the end of the study. In the intermediate and deep stroma of the H-E stained preparations, there was a void where the ICRS was originally located but then lost during the sectioning of the preparations (Figure 5**). This void changed in shape, perimeter, and area during the follow-up period. Cells lined the interface between the corneal stroma and the void where the inferior edges of the segment were present in situ (Figure 5,*). This area corresponded to the region of lamellar channel deposits seen on clinical examination. The morphology of these cells also changed over time. Descemet´s membrane and the endothelium did not show any structural changes. The complet process of wound healing after intrastromal corneal ring implantation will be the issue of another manuscript.

Histological findings in corneas with complications were represented in Figure 6. Characteristic endothelial-stroma scar secondary to a intraoperative posterior corneal perforation intro the antherior chamber (Figure 6A), neovascularization (Figure 6B) and a infiltrate of inflammatory cells around the ICRS (Figure 6C).
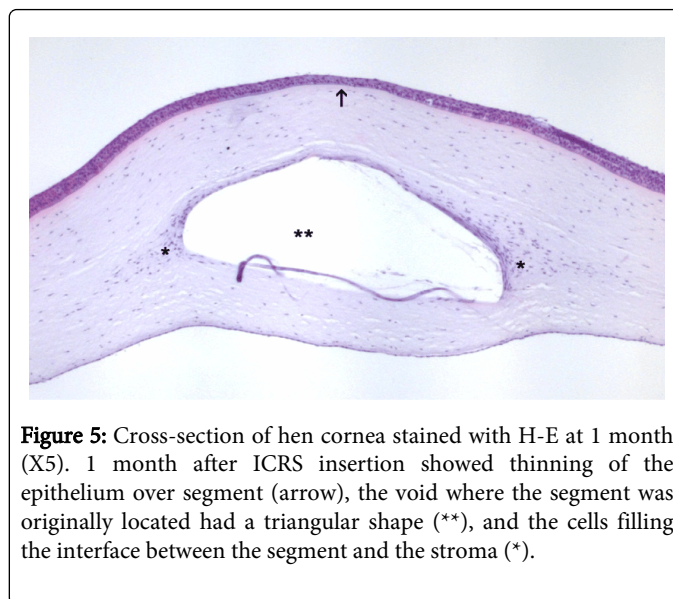

Figure 5: Cross-section of hen cornea stained with H-E at 1 month (X5). 1 month after ICRS insertion showed thinning of the epithelium over segment (arrow), the void where the segment was originally located had a triangular shape (**), and the cells filling the interface between the segment and the stroma (*).
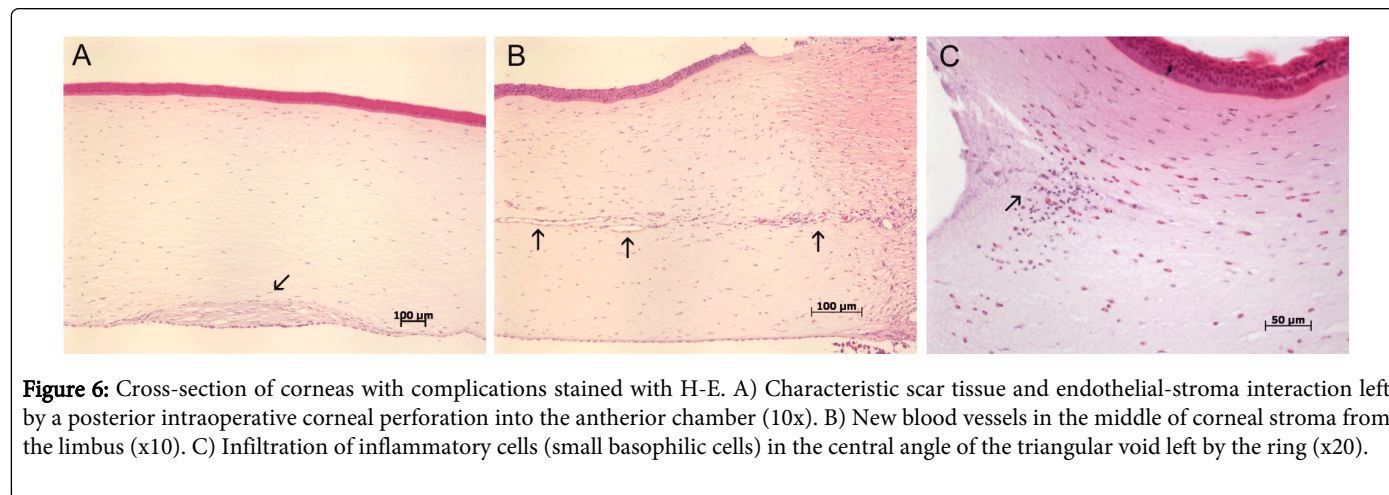

Figure 6: Cross-section of corneas with complications stained with H-E. A) Characteristic scar tissue and endothelial-stroma interaction left by a posterior intraoperative corneal perforation into the antherior chamber (10x). B) New blood vessels in the middle of corneal stroma from the limbus (x10). C) Infiltration of inflammatory cells (small basophilic cells) in the central angle of the triangular void left by the ring (x20).

Discussion

This is a preliminary study to assess the hen as an experimental animal model to train surgery of ICRS implantation and to future wound healing studies. In this study, we have performed the learning curve and described the clinical and optical outcomes of good follow up corneas after ICRS implantation. Many previous studies in humans have focused on the refractive, clinical, and optical events after ICRS implantation. To study the wound healing process, authors have used confocal microscopy, [17] anterior segment optical coherence tomography, [18,19] and scanning electron microscopy to analyze the explanted segments [12]. However these techniques cannot detect the morphology of the cells implicated at each time of follow-up to determine if they are keratocytes, fibroblasts, and/or myofibroblasts. Some histological studies of human corneas that were removed for keratoplasty due to ICRS complications or refractive failure have been reported. However, these studies do not established a temporal sequence of events, and the number of eyes analyzed was small [27,28]. For these reasons we thought it was necessary to develop an experimental animal model to study clinical, optical, and histological

events together throughout the wound healing process after Ferrara ICRS implantation in good and complicated eyes.

The rabbit was used as an experimental model for wound healing after ICRS implantation, [7] but there are differences between rabbits and humans in corneal anatomy and biomechanical properties, as well as in the healing process itself. Enucleated pig eyes have also been commonly used for surgical practice, but the difficulty in manipulating the living animal, along with the cost and the anatomical differences from human corneas also make them unsuitable as a model for training and long-term studies [29,30]. All of these reasons led us to propose the chicken as an experimental animal model for developing the ICRS surgical implantation technique with the learning curve and studying the post-surgical clinical and optical responses. The chicken is ethically acceptable, cheap, easy to handle, and the corneal anatomy with respect to layers and the distribution and wound healing response are similar to that of humans [20,21,31]. Nevertheless, our model has some drawbacks. First, the corneal dimensions are not exactly the same as those in humans. For this reason we had to create and adapt the surgical instruments for our animal model. Secondly, there are differences in the collagen arrangement [32] and accommodative mechanism, [24,25] although we believe that these would not interfere with the clinical and wound healing process.

The Ferrara ICRS chosen for this study all had the same size, arc, and thickness and were implanted at the same location in each cornea (inferotempotal quadrant) to make the measurements comparable between eyes. This location also coincide with the place where the ectasia is in the majority of the patients and where the majority of the segments are implanted [4,5]. We selected the thinnest segment recommended for humans to follow the Ferrara rule of segment implantation: "The thickness of the implanted segment should not be more than 50% of the corneal thickness in the ring track and the incision depth should be preferably set at 80% of the corneal thickness" [14]. The segment thickness was 150 μm, more than 50% of the hen central corneal thickness, but we estimated that it was less than 50% of the peripheral cornea thickness. We had difficulties in measuring the peripheral corneal thickness with ultrasound pachymetry due to the narrow anterior chamber of the hen. However, the measurements obtained were all more than 300 μm. Moreover, we implanted the segment at 71.2% of the corneal thickness (243.7 ± 24.0 μm) to avoid extrusions.

The incidence of complications in humans has been decreasing with more experience and especially with the use of the femtosecond laser [33,34]. Too deep or too superficial stromal tunnels, with too deep or too superficial implantation of the segments, segments implanted closely to the incisions and aggresive, powerful or in bad direction maneuvers are related to high incidence of complications, especially in first surgeries. It is important to know how to insert instruments and the segments along the deep stroma where the resistence is lower.In most recent studies, no complications were reported or were reported only in small numbers such as 3.8% in the latest Ferrara publication [5]. The incidence of complications in our study, 16% is similar to the first studies in humans [10,12] and could be attributed, as in those studies, to the learning curve and particularly in our experiments, to the adaptation of the surgery to our animal model. We also have the same type of complications as those described in humans. Femtosecond laser to segment implantation is not avaliable in the majority of the centers, for this reason the use of an experimental animal model could be suitable to reduce the learning curve and the incidence of the first complications with manual technique.

Lamellar channel deposits have been reported as a complication in some human trials [4]. Deposits are different from stromal haze. Stromal haze is described as a condition of mild anterior stroma opacification that occurs as a part of the normal wound healing response. Stromal haze has frequently been reported in the incision and surrounding the ICRS, and should be distinguished from intrastromal deposits that are only described around the segment.

Stromal deposits were reported in some studies from 7 days after surgery [22]. We likewise found deposits in our study at that time point, but the incidence was higher (28.4%). However, in other studies the early deposits appeared at a mean of 1 month after surgery, [35] and the authors stated that earlier deposits could be mistaken for haze around the channel. We disagree with this latter assessment because we were able to perceive little white speck-like deposits near the inner curvature that were different from the diffuse haze around the segment. The incidence of lamellar channel deposits in all studies increased over time. The incidence was related to the segment thickness and was inversely related to size of the channel where the segments were implanted [33,34]. The incidence of deposits varies in different studies from 12.5% in femtosecond implanted segment studies to the majority of the eyes in first studies [7,17,33,34]. However, in our animal model, 100% of the eyes presented intrastromal deposits at 3 months, a period that differed from other studies. Our animal model presented deposits located principally along the inner curvature of the segment at 1 and 2 months, which agrees with most long-term follow-up studies. However, we found that at 4 and 5 months, the deposits were mainly present along the external curvature of the segment and beneath it, locations that were not reported in other studies. This might be in part explained by differences in the morphology of the segments. In our case, using the Ferrara ICRS, the shape was triangular, but most wound healing studies after ICRS implantation were undertaken with hexagonal INTACS. Furthermore, these differences might be related to the involvement of more cells and the production of more new matrix during the wound healing process in the hen, which we believe might enable better understanding of the mechanism involved.

The severity of these deposits increased with time in all published studies [7,21]. In rabbits, two types of deposits were described. One had an oil drop appearance and the other, which appeared later, had a crystalline appearance [7]. In humans, different classifications have been described [17,22]. The most widely used classification is that by Ruckhofer et al. who designated 4 grades of deposits based on a qualitative description [22]. In our animal model, the evolution of deposits was slightly different. The deposits also increased over time from small and white in color at 1 month, to more confluent, larger and more yellow ones at 3 months. Later, they changed again to smaller, less confluent and white in color from 4 to 6 months, particularly those located under the segment. This could be related to the proliferation and differentiation of cells around the segment (date no shown in this manuscript).

Many studies in the literature have tried to describe the composition of these deposits, but it remains unknown. It is widely known that they are deposited in the empty space between the segment and the stroma where it is implanted. Most of the studies found new matrix synthesis, collagen disruption in addition to keratocytes, fibroblasts, or myofibroblasts [17,27,28]. We agree with these findings without specify the type of cells with our preliminary analysis of hematoxilin eosin stained preparations. However, more studies about wound healing should be performed to understand the

mechanism of this response specially in experimental animal models like the hen.

The refractive effects of ICRS have been widely studied in humans [5,6] and all have shown statistically significant flattening of the cornea [4,16]. This agrees with the expected change of curvature considering the mechanism of action of the ring segments described by Barraquer and Blavatslaya [4]. ICRS implantation can reduce sphere from 0.43 to 5 D and cylinder measurements from 0.75 to 2.88 D. The mean keratometric change with ICRS varies depending on the author and ICRS type, with values ranging from 2.14 to 9.60 D after Ferrara Ring implantation.4 For the hens in our study, we found an increase in the hyperopic refraction of 2.85 D, which remained stable during the 6 months of follow-up. These results agree well with those described in humans. Moreover, central cornea is not affected.

In summary, with hen as an experimental animal model, a beginner surgeon could experiment and discover with his own hands the specifics tips of intrastromal corneal ring segment surgery; how to direct instruments and segments along the specific depth without being too superficial or too deep, how to rotate the segment to the semicircular channell, how to know the specific strength needed to drive the instruments or segments in order to minimize the number of complications and have a more successful surgery.

In this study, an experimental animal model of ICRS implantation has been assessed with its learning curve and characterized by clinical, biophysical, and preliminary biological parameters. The majority of the optical and clinical events described in hens correlate with those described in humans. The differences regarding incidence, location, and severity of deposits should be studied to better understand the wound healing mechanism.

Acknowledgments

Financial Support

Conflict of Interest

The authors have no commercial relationship with any of the materials mentioned in the article. It was presented in part at the 2014 ARVO Annual Meeting, leading eye and Vision Research, May 4-8, 2014, in Orlando, Florida.

References

1. Romero-Jiménez M, Santodomingo-Rubido J, Wolffsohn JS (2010) Keratoconus: a review. Cont Lens Anterior Eye 33: 157-166.
2. Olson RJ, Pingree M, Ridges R, Lundergan ML, Alldredge C Jr, et al. (2000) Penetrating keratoplasty for keratoconus: a long-term review of results and complications. J Cataract Refract Surg 26: 987-991.
3. Wollensak G, Spoerl E, Seiler T (2003) Riboflavin/ultraviolet-a-induced collagen crosslinking for the treatment of keratoconus. Am J Ophthalmol 135: 620-627.
4. Piñero DP, Alio JL (2010) Intracorneal ring segments in ectatic corneal disease - a review. Clin Experiment Ophthalmol 38: 154-167.
5. Ferrara G, Torquetti L, Ferrara P, Merayo-Lloves J (2012) Intrastromal corneal ring segments: visual outcomes from a large case series. Clin Experiment Ophthalmol 40: 433-439.
6. Torquetti L, Berbel RF, Ferrara P (2009) Long-term follow-up of intrastromal corneal ring segments in keratoconus. J Cataract Refract Surg 35: 1768-1773.
7. Twa MD, Ruckhofer J, Kash RL, Costello M, Schanzlin DJ (2003) Histologic evaluation of corneal stroma in rabbits after intrastromal corneal ring implantation. Cornea 22: 146-152.
8. Ertan A, Colin J (2007) Intracorneal rings for keratoconus and keratectasia. J Cataract Refract Surg 33: 1303-1314.
9. Chan SM, Khan HN (2002) Reversibility and exchangeability of intrastromal corneal ring segments. J Cataract Refract Surg 28: 676-681.
10. Asbell PA, Uçakhan OO, Abbott RL, Assil KA, Burris TE, et al. (2001) Intrastomal corneal ring segments: reversibility of refractive effect. J Refract Surg 17: 25-31.
11. Levy J, Lifshitz T (2010) Keratitis after implantation of intrastromal corneal ring segments (intacs) aided by femtosecond laser for keratoconus correction: case report and description of the literature. Eur J Ophthalmol 20:780-784.
12. Ferrer C, Alió JL, Montañés AU, Pérez-Santonja JJ, del Rio MA, et al. (2010) Causes of intrastromal corneal ring segment explantation: clinicopathologic correlation analysis. J Cataract Refract Surg 36: 970-977.
13. Cosar CB, Sridhar MS, Sener B (2009) Late onset of deep corneal vascularization: a rare complication of intrastromal corneal ring segments for keratoconus. Eur J Ophthalmol 19: 298-300.
14. Torquetti L, Ferrara P (2010) Reasons for intrastromal corneal ring segment explantation. J Cataract Refract Surg 36: 2014.
15. Alió JL, Artola A, Hassanein A, Haroun H, Galal A (2005) One or 2 Intacs segments for the correction of keratoconus. J Cataract Refract Surg 31: 943-953.
16. Boxer Wachler BS, Christie JP, Chandra NS, Chou B, Korn T, et al. (2003) Intacs for keratoconus. Ophthalmology 110: 1031-1040.
17. Ruckhofer J, Böhnke M, Alzner E, Grabner G (2000) Confocal microscopy after implantation of intrastromal corneal ring segments. Ophthalmology 107: 2144-2151.
18. Pérez-Merino P, Ortiz S, Alejandre N, Jiménez-Alfaro I, Marcos S (2013) Quantitative OCT-based longitudinal evaluation of intracorneal ring segment implantation in keratoconus. Invest Ophthalmol Vis Sci 54: 6040-6051.
19. Gorgun E, Kucumen RB, Yenerel NM, Ciftci F (2012) Assessment of intrastromal corneal ring segment position with anterior segment optical coherence tomography. Ophthalmic Surg Lasers Imaging 43: 214-221.
20. Martínez-García MC, Merayo-Llovés J, Blanco-Mezquita T, Mar-Sardaña S (2006) Wound healing following refractive surgery in hens. Exp Eye Res 83: 728-735.
21. Merayo-Lloves J, Blanco-Mezquita T, Ibares-Frias L, Fabiani L, Alvarez-Barcia A, et al. (2010) Induction of controlled wound healing with PMMA segments in the deep stroma in corneas of hens. Eur J Ophthalmol 20: 62-70.
22. Ruckhofer J, Twa MD, Schanzlin DJ (2000) Clinical characteristics of lamellar channel deposits after implantation of intacs. J Cataract Refract Surg 26: 1473-1479.
23. Fantes FE, Hanna KD, Waring GO 3rd, Pouliquen Y, Thompson KP, et al. (1990) Wound healing after excimer laser keratomileusis (photorefractive keratectomy) in monkeys. Arch Ophthalmol 108: 665-675.
24. Schaeffel F, Glasser A, Howland HC (1988) Accommodation, refractive error and eye growth in chickens. Vision Res 28: 639-657.
25. Schaeffel F, Howland HC (1987) Corneal accommodation in chick and pigeon. J Comp Physiol A 160: 375-384.

26. Mar S, Martinez-García MC, Blanco-Mezquita T, Torres RM, and Merayo-Lloves J (2009) Meassurement of correlation between transmission and scattering during wound healing in hen corneas. Journal of modern Optics 56:1-8.

27. Samimi S, Leger F, Touboul D, Colin J (2007) Histopathological findings after intracorneal ring segment implantation in keratoconic human corneas. J Cataract Refract Surg 33: 247-253.

28. Maguen E, Rabinowitz YS, Regev L, Saghizadeh M, Sasaki T et al. (2008) Alterations of extracellular matrix components and proteinases in human corneal buttons with INTACS for post-laser in situ keratomileusis keratectasia and keratoconus. Cornea 27: 565-573.

29. Al-Amry M, Alkatan HM (2011) Histopathologic findings in two cases with history of intrastromal corneal ring segments insertion. Middle East Afr J Ophthalmol 18: 317-319.

30. Sweatt AJ, Ford JG, Davis RM (1999) Wound healing following anterior keratectomy and lamellar keratoplasty in the pig. J Refract Surg 15: 636-647.

31. Fowler WC, Chang DH, Roberts BC, Zarovnaya EL, Proia AD (2004) A new paradigm for corneal wound healing research: the white leghorn chicken (Gallus gallus domesticus). Curr Eye Res 28: 241-250.

32. Boote C, Hayes S, Jones S, Quantock AJ, Hocking PM, et al. (2008) Collagen organization in the chicken cornea and structural alterations in the retinopathy, globe enlarged (rge) phenotype--an X-ray diffraction study. J Struct Biol 161: 1-8.

33. Ertan A, Kamburoglu G, Akgun U (2007) Comparison of outcomes of 2 channel sizes for intrastromal ring segment implantation with a femtosecond laser in eyes with keratoconus. J Cataract Refract Surg 33: 648-653.

34. Ratkay-Traub I, Ferincz IE, Juhasz T, Kurtz RM, Krueger RR (2003) First clinical results with the femtosecond neodynium-glass laser in refractive surgery. J Refract Surg 19: 94-103.

35. Assil KK, Barrett AM, Fouraker BD, Schanzlin DJ (1995) One-year results of the intrastromal corneal ring in nonfunctional human eyes. Intrastromal Corneal Ring Study Group. Arch Ophthalmol 113: 159-167.